Materials Science and Engineering B 154–155 (2008) 20–23

Contents lists available at ScienceDirect

Materials Science and Engineering B

journal homepage: www.elsevier.com/locate/mseb

Simulation of dopant diffusion and activation during flash lamp annealing

Christoph Zechner[a], Dmitri Matveev[a,*], Nikolas Zographos[a], Wilfried Lerch[b], Silke Paul[b]

[a] Synopsys Switzerland LLC, Affolternstrasse 52, CH-8050 Zurich, Switzerland
[b] Mattson Thermal Products GmbH, Daimlerstrasse 10, D-89160 Dornstadt, Germany

ARTICLE INFO

Article history:
Received 5 May 2008
Received in revised form
29 September 2008
Accepted 9 October 2008

Keywords:
FLA
Diffusion
Activation
Simulation

ABSTRACT

A set of advanced models implemented into the simulator *Sentaurus Process* was applied to simulate ultra shallow junction formation by flash lamp annealing (FLA). The full path transient enhanced diffusion model includes equations for small interstitial clusters (I_2, I_3, I_4), {3 1 1} defects and dislocation loops. A dopant-point defect clustering model is used for dopant activation simulation. Several cluster types are considered: B_2, B_2I, B_2I_2, B_3I, B_3I_2, B_3I_3 for boron and As_2, As_2V, As_3, As_3V, As_4, As_4V for arsenic. Different point defect and dopant-point defect pair charge states are taken into account to obtain accurate results in the high doping level region. The flux expressions in the three-phase segregation model include a dependence on the doping level and point defect supersaturation. The FLA process was performed at various peak temperatures in a Mattson Millios™ fRTP™ system. The measured wafer temperature as a function of time allowed us to simulate the transient processes with a high accuracy. A good agreement between secondary ion mass spectroscopy (SIMS) and simulated profiles was achieved. The sheet resistance dependence on the FLA peak temperature was reproduced successfully.

1. Introduction

Flash lamp annealing (FLA) is an attractive technique for the formation of ultra shallow profiles [1,2]. The main FLA advantage is a high dopant activation level together with a limited diffusion. Simulation of dopant diffusion and activation during FLA requires the use of complex models taking an interaction between dopants, point defects and extended defects into account because of low thermal budget. In this paper, we present new models for dopant-point defect clustering and segregation which were successfully applied to FLA simulation.

2. Models

An accurate simulation of the transient enhanced diffusion (TED) is very important in the case of low thermal budget annealing. In this work, we use the previously developed full path TED model [3,4]. The model includes equations for small interstitial clusters (I_2, I_3, I_4), {3 1 1} defects and dislocation loops. It was successfully used for TED simulation in the wide range of process conditions.

Experimental data as well as ab-initio calculations show that dopants can be deactivated by the dopant-point defect cluster formation [5]. In our new activation model, clusters can be formed by different type reactions:

$$A^z + AX^m \Leftrightarrow A_2X + (-z-m)e$$

$$AX^m + AX^k \Leftrightarrow A_2X_2 + (-m-k)e$$

$$AX^m + AY^k \Leftrightarrow A_2 + (-m-k)e$$

$$CL_1 + X^m \Leftrightarrow CL_2 + (-m)e$$

$$CL_1 + AX^m \Leftrightarrow CL_2 + (-m)e$$

where A is the substitutional dopant, X is the mobile point defect, AX and AY are the mobile dopant-point defect pairs, CL_1 and CL_2 are dopant clusters. z, m and k denote the charge states. All clusters are electrically neutral and immobile. The forward clustering reactions are assumed to be diffusion limited, and the rates for the backward ones are derived from the calculated equilibrium state. The reaction rates are summed up over all the point defect and dopant-point defect pair charge states. For example, the obtained equation for the reaction between cluster and point defect $CL_1 + X \Leftrightarrow CL_2$ has the following form

$$R = 4\pi a f D_X \frac{C_{CL1}C_X - C_{CL2}C_X^* N_{CL1}}{N_{CL2}} \exp\left(\frac{E_{CL1} - E_{CL2}}{k_B T}\right)$$

where C_X is the point defect concentration, C_X^* is the point defect equilibrium concentration, C_{CL1} and C_{CL2} are the cluster concen-

* Corresponding author. Tel.: +41 44 5671560.
E-mail address: matveev@synopsys.com (D. Matveev).

0921-5107/$ – see front matter © 2008 Elsevier B.V. All rights reserved.
doi:10.1016/j.mseb.2008.10.005

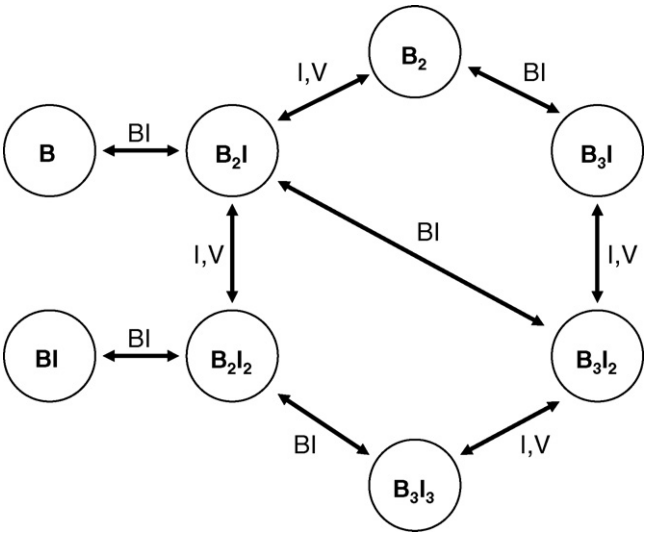

Fig. 1. Reaction pathway for the BICs model.

trations, D_X is the point defect diffusivity, N_{CL1} and N_{CL2} are the numbers of possible cluster configurations, E_{CL1} and E_{CL2} are the cluster formation energies, a is the silicon lattice spacing, f is the reaction capture radius factor.

The developed model was applied to simulate BICs and As–V cluster formation. The proposed reaction pathway for boron is shown in Fig. 1. Similar to the BIC model presented in [7], the most stable B cluster in our model is B_3I, followed by B_3I_2. B clusters with four or more B atoms are not included in order to keep the number of equations small. Arsenic clustering reactions were defined according to the model published by Pinacho et al. [6] (Fig. 2). The most stable As cluster is As_4V, as suggested by ab-initio simulations [8].

The model for B and As clustering contains several parameters for each cluster: E_{CL}, N_{CL}, f. For the purpose of calibration, only the formation energies E_{CL}, which are the most important model parameters, were optimized, whereas N_{CL} and f were kept at initially fixed values. During calibration, the agreement between simulation results and a selection of SIMS data (including data from furnace anneals, RTA and spike anneals for various implant conditions) was optimized. In this method, the formation energy of the most stable clusters determines the active dopant concentration which is reached in long time anneals in highly doped regions. The FLA data presented in this work were not used in the original model calibration. The model parameters are summarized in Table 1.

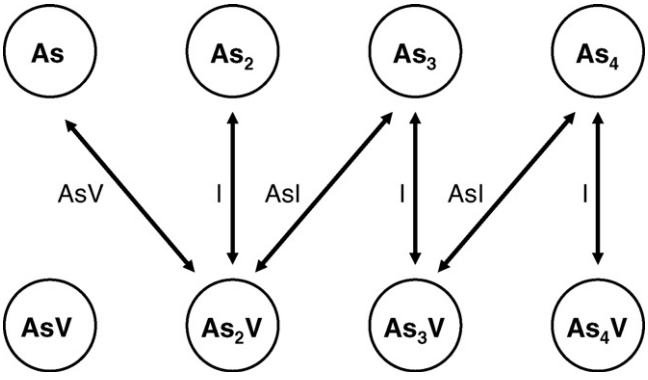

Fig. 2. Reaction pathway for the As–V clustering model.

Table 1
Parameters used for the boron-interstitial and the arsenic-vacancy clustering model. Negative or small positive formation energies correspond to stable clusters. E_{CL}, formation energy. N_{CL}, degeneracy. f, capture radius factor (capture radius divided by the lattice constant).

Cluster	E_{CL} (eV)	N_{CL} [1]	f [1]
BICs			
B_2	0.7	2.0	1.3
B_2I	0.976	4.0	1.5
B_2I_2	1.108	4.0	1.7
B_3I	−0.06	4.0	1.7
B_3I_2	0.14	3.0	2.0
B_3I_3	1.1	4.0	2.0
AsV clusters			
As_2	0.8	2.0	1.0
As_2V	0.7	4.0	1.0
As_3	0.6	2.0	1.0
As_3V	0.25	4.0	1.0
As_4	0.5	2.0	1.0
As_4V	0.1	4.4	1.0

For ultra shallow junction formation, the surface influence on dopant atom migration is very important. We developed a three-phase segregation model, based on [9], which accurately describes the dopant interface trapping and emission processes in the regions with high doping level and interstitial supersaturation. In contrast to [9], in our new model, only mobile dopant-defect pairs can be captured to or released from the interface. The possible reactions are:

$$AX^m + me \Leftrightarrow A_{\text{int}} + X^0$$

where A_{int} is the dopant atom captured in the interface, X^0 is the neutral point defect. For the oxide/silicon interface, the derived equation for the pair flux from the silicon side into the interface can be written as follow

$$\text{Flux}_{AX} = \frac{f_{AX}t}{C_X^{0*}}\left[\frac{C_{AX}(n/n_i)^z(C_{\max}-C_{A\text{int}})}{\sum(k_X^j\, k_{AX}^j(n/n_i)^{-j})} - C_{A\text{int}}C_X^0(e/t)\,C_{ss}\right]$$

where C_X^0 is the neutral point defect concentration, C_X^{0*} is the neutral point defect equilibrium concentration, C_{AX} is the dopant-point defect pair concentration, $C_{A\text{int}}$ is the concentration of dopant captured in the interface, $C_{\max}$ is the maximum concentration of interface traps, C_{ss} is the dopant solid solubility in silicon, n is the electron concentration, n_i is the intrinsic electron concentration, k_X^j and k_{AX}^j are the point defect ionization coefficient and dopant pairing constant for the charge state j. t, e and f_{AX} denote the trapping rate, emission rate and the flux fraction due to AX pairs trapping/detrapping, respectively. It should be noted that the obtained flux expression depends on the doping level and point defect concentration. It allows an accurate simulation of dopant segregation in the region with a high active dopant concentration and interstitial supersaturation.

All models and parameters described in this section are included in the Advanced Calibration [10] set of models of the process simulator Sentaurus Process.

3. Experiment

Experiments were performed at Mattson Thermal Products. Wafers were implanted with boron or arsenic at energy of 0.5 keV and with a dose of $10^{15}\,\text{cm}^{-2}$ using an Applied Materials Quantum batch implanter. Subsequently, samples were annealed in a Mattson Millios™ fRTP™ system at 1275, 1300 and 1325 °C peak temperatures with intermediate temperatures of 700 °C for boron and 750 °C for arsenic. The actual wafer temperature as a

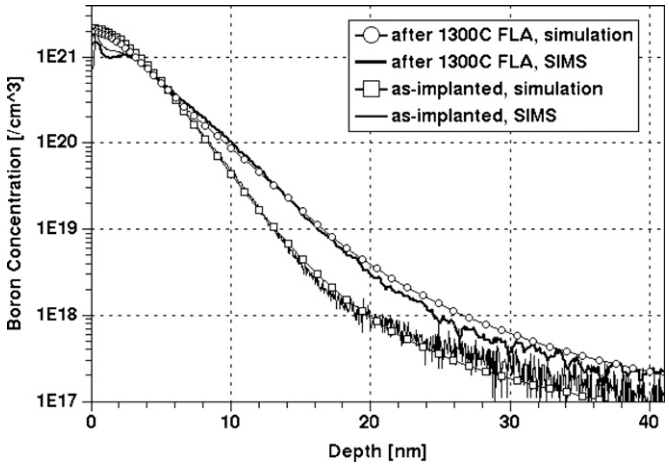

Fig. 3. Comparison of SIMS (lines without symbols) and simulated (lines with symbols) boron profiles.

function of time was measured [11] and then used in simulations. It allowed us to simulate transient processes with a high accuracy. After processing, the depth profiles were measured by SIMS using a CAMECA 4600 instrument. The sheet resistance measurements were performed by a KLA-Tencor RS-100 four point probe.

4. Results and discussion

A comparison of simulated and SIMS profiles is presented in Figs. 3–4. The as-implanted profiles were adjusted to the corresponding SIMS data. Default Advanced Calibration parameters were used without any change for boron diffusion and activation simulation. In the arsenic case, the capturing rate for the reaction $As_2V + I \Leftrightarrow As_2$ (Fig. 2) was reduced for fine-tuning, but all other parameters were unchanged.

A good agreement between simulation and SIMS was achieved. Some disagreement is observed for arsenic profiles at the surface (Fig. 4). The reason for it is, most probably, dopant redistribution during the solid phase epitaxial regrowth (SPER). In the experiment, during SPER, arsenic is pushed towards the surface by a snow-plow effect at the moving amorphous/crystalline interface. It results in the profile peak shift towards the surface, observed in SIMS [2]. This particular effect is not included in our models. Nevertheless, the change of junction depth during FLA is well reproduced (Fig. 4).

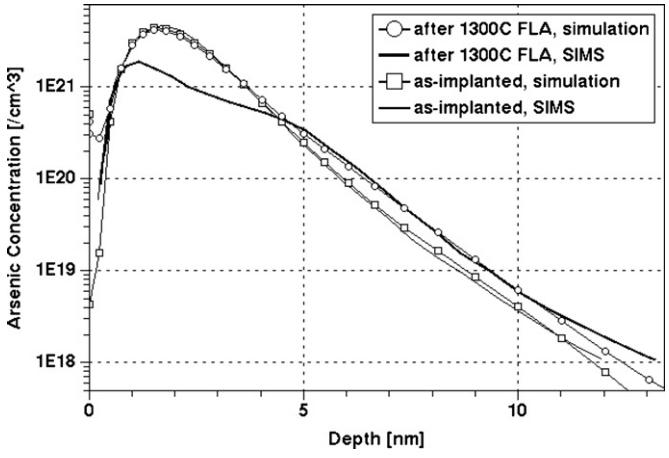

Fig. 4. Comparison of SIMS (lines without symbols) and simulated (lines with symbols) arsenic profiles.

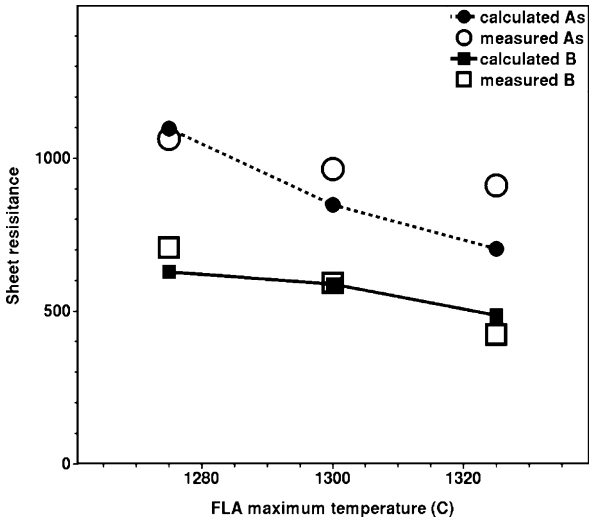

Fig. 5. Comparison of measured (open squares for boron, open circles for arsenic) and calculated (closed squares and solid line for boron, closed circles and dashed line for arsenic) sheet resistance (Ω/sq.) for different FLA maximum temperatures.

Calculated and measured sheet resistance values are shown in Fig. 5. There is a good agreement between simulations and experiments for boron. An agreement for arsenic is also good, although the calculated resistance dependence on the peak FLA temperature is stronger than the measured one.

5. Conclusions

New dopant activation and segregation models were developed. An interaction of dopant and clusters with point defects and dopant-defect pairs at different charge states is taken into account in the activation model. The dopant interface trapping process can be simulated accurately in the region with high doping level and interstitial supersaturation using the proposed segregation model. The activation, segregation and previously developed full path TED models were successfully applied to simulate diffusion and activation of boron and arsenic during FLA. A good agreement between SIMS and simulated profiles was achieved. The sheet resistance dependence on the FLA peak temperature was reproduced successfully.

Acknowledgments

The authors would like to thank J. Gelpey, S. McCoy and J. Chan of Mattson Thermal Products for their effort to measure the time/temperature profiles in high resolution needed for this work as well as for the wafer processing.

References

[1] W. Lerch, S. Paul, J. Niess, S. McCoy, T. Selinger, J. Gelpey, F. Cristiano, F. Severac, M. Gavelle, S. Boninelli, P. Pichler, D. Bolze, Mater. Sci. Eng. B 124–125 (2005) 24–31.
[2] W. Lerch, S. Paul, J. Niess, S. McCoy, J. Gelpey, D. Bolze, F. Cristiano, F. Severac, P.F. Fazzini, A. Martinez, P. Pichler, Proceedings of the IEEE Electron Devices Society: 15th IEEE International Conference on Advanced Thermal Processing of Semiconductors 2007, October 2–5, 2007, Catania, Italy, RTP 2007, Piscataway, NJ, IEEE, 2007, pp. 191–196.
[3] C. Zechner, N. Zographos, D. Matveev, A. Erlebach, Mater. Sci. Eng. B 124–125 (2005) 401–403.
[4] N. Zographos, C. Zechner, I. S Avci, in: S. Ashok, P. Kiesel, J. Chevallier, T. Ogino (Eds.), Material Research Society Symposium Proceedings 994: Semiconductor

Defect Engineering – Materials Synthetic Structures and Devices II, 2007, 0994, F10-01.
[5] P. Pichler, Intrinsic Point Defects, Impurities, and Their Diffusion in Silicon, Springer-Verlag, Vienna, 2004.
[6] R. Pinacho, M. Jaraiz, P. Castrillo, I. Martin-Bragado, J.E. Rubio, J. Barbolla, Appl. Phys. Lett. 86 (2005) 252103.
[7] J. Schermer, A. Martinez-Limia, P. Pichler, C. Zechner, W. Lerch, S. Paul, Solid State Electron. 52 (2008) 1424–1429.
[8] S.A. Harrison, T.F. Edgar, G.S. Hwang, Electrochem. Solid State Lett. 9 (12) (2006) G354–G357.
[9] Y.-S. Oh, D.E. Ward, IEDM Technical Digest, San Francisco, CA, USA, December, 1998, pp. 509–512.
[10] Advanced Calibration User Manual, Synopsys Inc., December, 2007.
[11] W. Lerch, S. Paul, J. Niess, S. McCoy, J. Gelpey, F. Cristiano, F. Severac, P. Fazzini, A. Martinez-Limia, P. Pichler, H. Kheyrandish, D. Bolze (2008) (this conference).